JOURNAL OF VIROLOGY, Oct. 1997, p. 8066–8072 Vol. 71, No. 10
0022-538X/97/$04.00+0


# Biochemical Characterization of a Smaller Form of Recombinant Norwalk Virus Capsids Assembled in Insect Cells

LAURA J. WHITE, MICHELE E. HARDY, AND MARY K. ESTES*

*Division of Molecular Virology, Baylor College of Medicine, Houston, Texas 77030*

Received 3 January 1997/Accepted 17 June 1997

**The expression of the single capsid protein of Norwalk virus (NV) in *Spodoptera frugiperda* (Sf9) insect cells infected with recombinant baculovirus results in the assembly of virus-like particles (VLPs) of two sizes, the predominant 38-nm, or virion-size VLPs, and smaller, 23-nm VLPs. Here we describe the purification and biochemical characterization of the 23-nm VLPs. The 23-nm VLPs were purified to 95% homogeneity from the medium of Sf9 cultures by isopycnic CsCl gradient centrifugation followed by rate-zonal centrifugation in sucrose gradients. The compositions of the purified 23- and 38-nm VLPs were compared by sodium dodecyl sulfate-polyacrylamide gel electrophoresis and protein immunoblots. VLPs of both sizes showed a doublet at 58 kDa, the size of the full-length capsid protein. Upon alkaline treatment, the 23-nm VLPs underwent dissociation into soluble intermediates that were able to reassemble into 23- and 38-nm VLPs upon dialysis, suggesting that the assembly of both types of structures has a common pathway. Antigenic and biochemical properties of the 38- and 23-nm VLPs were examined and found to be conserved. Immunoprecipitation assays using polyclonal and monoclonal antibodies indicated that immunodominant epitopes on the capsid protein as well as conformational epitopes are conserved in the two types of particles. The trypsin cleavage site at residue 227 was protected in the assembled particles of both sizes but exposed after alkaline dissociation. These results, and the conservation of the binding activity of both forms of recombinant NV VLPs to cultured cells (L. J. White, J. M. Ball, M. E. Hardy, T. N. Tanaka, N. Kitamoto, and M. K. Estes, J. Virol. 70:6589–6597, 1996), suggest that the tertiary folding of the capsid protein responsible for these properties is conserved in the two structures. We hypothesize that the 23-nm VLPs are formed when 60 units of the NV capsid protein assembles into a structure with T=1 symmetry.**

Norwalk virus (NV) is a prototype strain of human caliciviruses, a group of pathogens responsible for outbreaks of gastroenteritis in humans (8). Norwalk virus is a small icosahedral virus composed of a single structural protein that contains a single-stranded plus-sense RNA genome of about 7.7 kb (20). This single polypeptide must encode all the functional entities required for NV structural integrity, infectivity, and immunogenicity. Study of this group of viruses has been hampered by the low amounts of virus in stool samples from infected individuals, along with the absence of a cell culture system and an animal model to propagate the virus (8).

The capsid proteins from several strains of human caliciviruses including NV (18), Mexico virus (17), Lordsdale virus (5), Toronto virus (21), Snow Mountain agent (11), and human calicivirus Sapporo (22) have been expressed in insect cells infected with recombinant baculoviruses. The capsid proteins from these viruses spontaneously assemble into empty virus-like particles (VLPs) that are released into the medium of the insect cell cultures from which they can be purified usually in high yields. In preparations of recombinant NV (rNV) VLPs (28) and recombinant Mexico virus VLPs (17) expressed in insect cell cultures, two sizes of particles have been found; the major fraction has a diameter of approximately 38 nm as determined by electron cryomicroscopy (24), while a small proportion of particles has a smaller diameter reported to be approximately 19 nm (28), 15 to 20 nm (17), or 23 nm (this study; see below). Particles of two sizes (35 to 40 and 15 to 20 nm) were also observed by immunoelectron microscopy in stool samples from patients infected with Otofuke agent (a human calicivirus present in stools during an outbreak of diarrhea in Japan) (27). The 38-nm rNV VLPs have been well characterized antigenically and morphologically (18), and the three-dimensional structure has been determined to a resolution of 2.2 nm by electron cryomicroscopy and computer image processing techniques (24). These studies revealed that the 38-nm rNV VLPs fold into T=3 icosahedral structures formed by 180 copies of the capsid protein. There are 90 arch-like capsomers at the local and strict twofold axes.

The self-assembly of viral capsids composed of a single structural protein into more than one structure has been described for icosahedral T=3 RNA plant viruses. The capsid proteins from southern bean mosaic virus (SBMV) (16, 25), turnip crinkle virus (26), alfalfa mosaic virus (9), and brome mosaic virus (4) are able to self-assemble in vitro into T=3 or smaller T=1 structures depending on factors such as trypsin digestion, the presence and size of the RNA genome, the presence of divalent cations, the ionic strength, and the pH.

The involvement of only one structural protein in the formation of the NV capsids, along with the availability of high-resolution structural data (24) and the ability of the capsid protein to dissociate and reassemble in vitro (14; also, this study), makes NV a good tool for morphogenesis studies of small icosahedral animal viruses. The biochemical and structural characterization of different forms of empty rNV VLPs may be helpful for evaluating the protein-protein interactions that govern assembly independently from the influence of protein-RNA interactions.

This paper describes the purification and biochemical characterization of the smaller 23-nm rNV VLPs assembled in vivo in insect cell cultures. Specifically, we analyzed the protein

* Corresponding author. Phone: (713) 798-3585. Fax: (713) 798-3586. E-mail: mestes@bcm.tmc.edu.

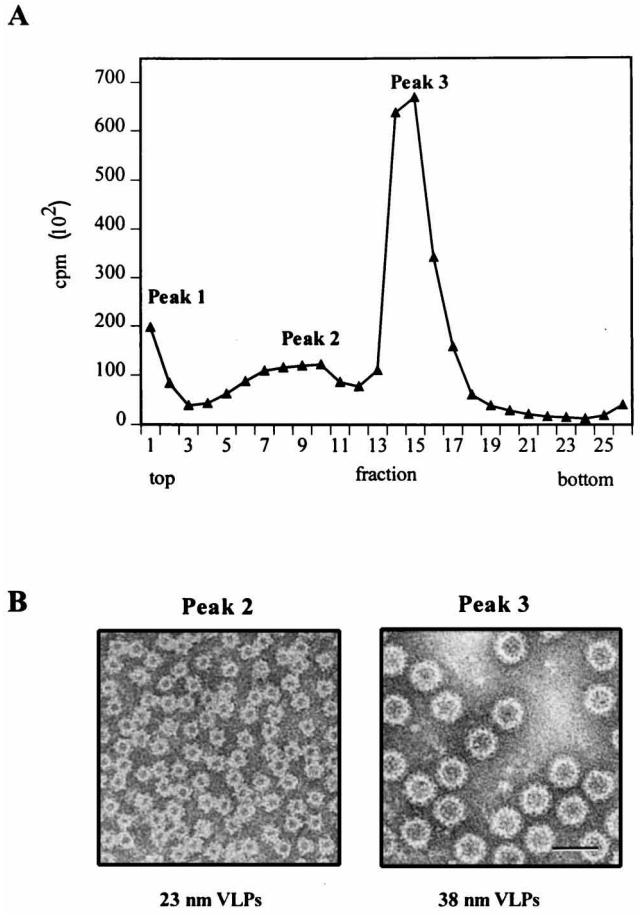


FIG. 1. Sedimentation of rNV VLPs on sucrose gradients. Preparations of VLPs separate into soluble capsid protein (peak 1), 23-nm VLPs (peak 2), and 38-nm VLPs (peak 3). (A) $^{35}$S-labeled rNV VLPs were pelleted for 2 h at 26,000 rpm in a Beckman SW28 rotor at 4°C from the medium of infected Sf9 cell cultures 7 days after infection and suspended in 0.01 M PBS, pH 7.2. The VLPs were then centrifuged in a CsCl isopycnic gradient and banded at a density of 1.31 g/cm$^3$. The VLPs collected in the band were pelleted for 2 h at 26,000 rpm in a Beckman SW28 rotor at 4°C and then sedimented in a five-step discontinuous 5 to 25% (wt/vol) sucrose gradient for 3.5 h at 35,000 rpm in a Beckman SW41 rotor at 4°C. Fractions were collected from the top, and radioactivity from each fraction was measured by liquid scintillation spectrometry. (B) Electron micrographs of purified particles in peaks 2 and 3. Fractions forming peaks 2 and 3 were pooled separately and concentrated by pelleting for 2 h at 26,000 rpm in a Beckman SW28 rotor at 4°C. Pelleted rNV VLPs were suspended in 0.01 M PBS, pH 7.2, and analyzed by negative-stain electron microscopy. Carbon-coated collodion 400-mesh grids were layered on top of 10 μl of the sample on Parafilm and incubated for 10 min at room temperature; excess fluid was removed with the edge of a filter paper disk, and the grids were washed with 10 μl of milli-Q water and stained for 30 s with 1% ammonium molybdate, pH 5.5. Bar, 50 nm.

composition, susceptibility to protease treatment, surface and antigenic properties, and the products of in vitro dissociation-reassembly of the 23-nm VLPs compared to the 38-nm VLPs.

**Purification of 23- and 38-nm VLPs.** Metabolically radiolabeled (Trans $^{35}$S-label; ICN, Irvine Calif.) 23- and 38-nm VLPs were purified separately from the media of Sf9 cell cultures infected with recombinant baculovirus (Bac-rNV C8) (18). Sf9 cells were infected and the culture medium was harvested as described earlier (28). The VLPs were concentrated from the media by ultracentrifugation followed by isopycnic CsCl gradient centrifugation (1.362 g/cm$^3$), where particles of both sizes banded at the same density of 1.31 g/ml. This mixed population of rNV VLPs contained predominantly 38-nm particles. The proportion of smaller-size VLPs varied from one preparation to another, being absent or undetectable in some preparations and representing up to 30% of the particles in others. To separate the two sizes of particles, the VLPs in the CsCl band were concentrated by ultracentrifugation and separated by rate-zonal centrifugation on a discontinuous 5 to 25% (wt/vol) sucrose gradient. The gradients were fractionated, and aliquots of each fraction were analyzed by scintillation counting. Three peaks of radioactivity were detected (Fig. 1A). The fractions forming peaks 2 and 3 were pooled separately, and the VLPs were concentrated by ultracentrifugation and suspended in 0.01 M PBS, pH 7.2. Aliquots from each of the three peaks were prepared for electron microscopic analysis by negative staining with 1% ammonium molybdate, pH 5.5. The diameters of the rNV VLPs were measured in electron microscopic negatives at a magnification of ×39,000. The material in peak 1, located at the top of the gradient, did not contain any particles detectable by electron microscopy, in agreement with peak 1 being soluble protein. Peak 2 contained VLPs with a diameter of 23.3 ± 0.73 nm, and peak 3 contained VLPs with a diameter of 34 ± 1.97 nm (Fig. 1B). By electron cryomicroscopy, the larger VLPs measured 38 nm (24). Electron microscopy analysis by negative-stain procedures gives particle sizes smaller than those observed by high-resolution structural analysis (23). Based on this, we predict that the actual size of the small particles measured by electron cryomicroscopy will be 26 to 27 nm. The sizes reported earlier for the smaller rNV VLPs by negative-stain techniques were 19 nm (28) and 15 to 20 nm (17), and the smaller "empty" particles in stool samples from patients infected with Otofuke agent were 15 to 20 nm (27). The difference between these sizes and our current measurement of 23 nm may be related to differences in the stain used, its concentration, and pH. The overall morphology of the 23-nm VLPs was similar to that of the 38-nm VLPs. The particles appeared empty, with protrusions similar to those in the images of 38-nm VLPs.

**Both 23- and 38-nm VLPs are composed of the 58K capsid protein.** To determine whether the smaller capsids were

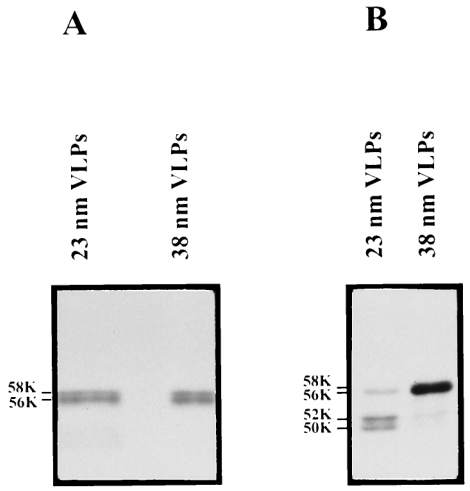


FIG. 2. VLPs with a diameter of 38 or 23 nm are composed predominantly of the 58K capsid protein. (A) The protein composition of VLPs purified as indicated in the legend to Fig. 1 was determined by SDS–10% PAGE. Protease inhibitors (aprotinin and leupeptin at 0.5 μg/ml each) were used throughout the purification procedure. Samples were boiled for 2 min, and equal amounts of radioactivity (counts per minute) were loaded onto the gel. Bands were visualized by autoradiography. (B) Protein analysis by SDS–12% PAGE of 23- and 38-nm VLPs purified and stored in the absence of protease inhibitors.

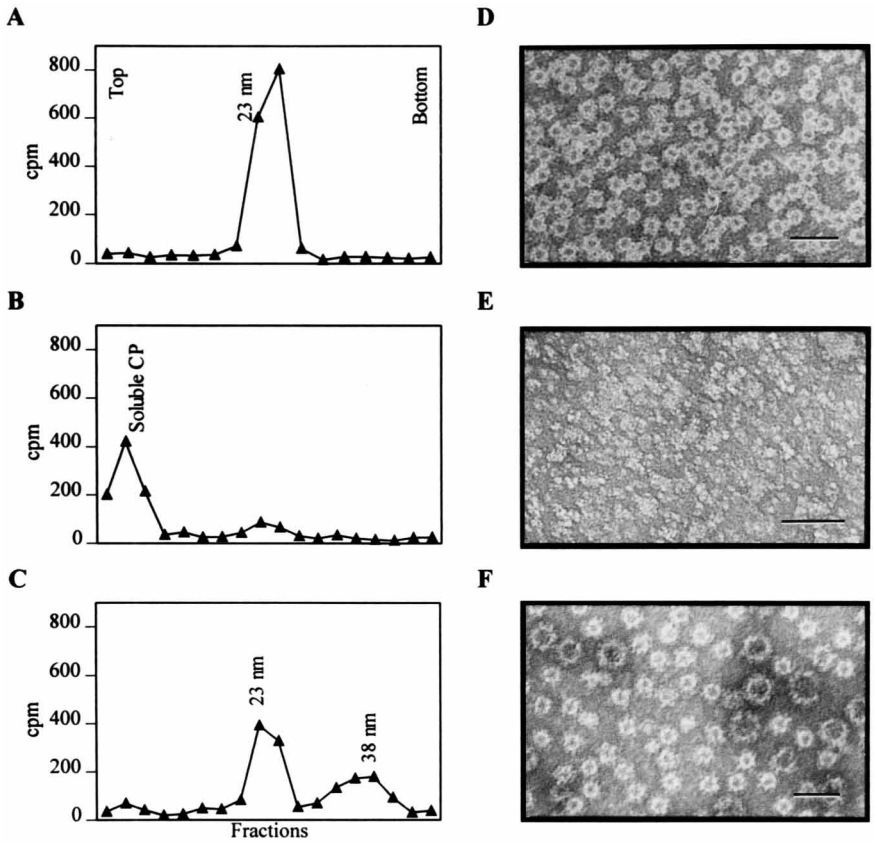


FIG. 3. In vitro disassembly-reassembly of 23-nm VLPs makes 23- and 38-nm VLPs. (A to C) Rate-zonal centrifugation on a discontinuous 5 to 25% (wt/vol) sucrose gradient made in 0.1 M phosphate buffer, pH 6.0 (A and C) or in 50 mM Tris-HCl, pH 8.9 (B) was used to characterize the products of the disassembly and reassembly of the 23-nm VLPs. The gradients were centrifuged for 1.5 h in a Beckman TLS55 rotor at 35,000 rpm at 4°C. Fractions were collected by bottom puncture, and the radioactivity was quantitated by scintillation counting. (A) Twenty-three-nanometer VLPs purified as indicated in the legend to Fig. 1; (B) purified 23-nm VLPs after treatment with 50 mM Tris, pH 8.9, at 4°C overnight; (C) alkaline-treated 23-nm VLPs after dialysis against 0.1 M phosphate buffer, pH 6.0, at 4°C; (D to F) electron micrographs of purified 23-nm VLPs corresponding to the ones characterized in panels A to C, respectively. Negative staining was performed as indicated in the legend to Fig. 1. Bars, 50 nm. CP, capsid protein.

formed by the intact NV capsid protein or by a cleaved or degraded fragment of this protein, 23- and 38-nm VLPs that were purified and stored in the presence of the protease inhibitors aprotinin (Sigma, St. Louis, Mo.) (0.5 μg/ml) and leupeptin (Sigma) (0.5 μg/ml) were analyzed by sodium dodecyl sulfate–polyacrylamide gel electrophoresis (SDS–PAGE) (Fig. 2A). VLPs of both sizes showed the same protein composition pattern, represented by a doublet at ~58 kDa. The smaller protein in the doublet (~56 kDa) is often seen in purified preparations of 38-nm VLPs, even when protease inhibitors are present during purification, and is likely an early cleavage product of the capsid protein within Sf9 cells. In overexposed gels, the 23-nm VLPs showed two smaller bands with approximate molecular weights of 52,000 and 50,000 (data not shown). The two smaller bands were not present in preparations of 38-nm VLPs purified simultaneously. Upon storage in the absence of protease inhibitors, the capsid protein was less stable in the 23-nm VLPs than in the 38-nm VLPs, as shown by a more rapid degradation of the 58-kDa (58K) protein into the 56K, 52K, and 50K cleavage products (Fig. 2B); these cleavage products, specifically the 52K and 50K products, appeared more slowly in the 38-nm VLPs. The higher instability of the 58K capsid protein in the 23-nm VLPs does not correlate with a higher instability of the particles, which remain intact in phosphate-buffered saline (PBS), pH 7.2, at 4°C for several months. The smaller proteins were related to the NV capsid protein based on reactivity with rabbit anti-rNV sera in Western blot (data not shown). The cleaved fragments reacted with an NV peptide antiserum directed against the C-terminal 15 residues of the NV capsid protein, suggesting that these fragments are cleaved in their N terminus. These observations suggest that the 58K capsid protein in the 23-nm VLPs is more susceptible to degradation of the N-terminal residues than the 58K capsid protein in the 38-nm VLPs.

**In vitro disassembly-reassembly of 23-nm VLPs results in 23- and 38-nm VLPs and occurs through common soluble intermediates.** To begin to understand the morphogenesis of the 23-nm VLPs, experiments on in vitro dissociation and reassembly of the 23-nm VLPs were performed. Purified 23-nm VLPs (0.3 to 1 mg/ml) were dissociated into soluble intermediates by alkaline treatment (50 mM Tris HCl, pH 8.9; overnight at 4°C) as described previously (13). Complete dissociation of the particles into soluble protein was shown by a shift of the radiolabeled peak of rNV VLPs from the center to the top of a 5 to 25% (wt/vol) sucrose gradient (Fig. 3A and B) and by the disappearance of particles examined by negative-stain electron microscopy (Fig. 3D and E). The soluble capsid protein was then dialyzed against 0.1 M phosphate buffer, pH 6.0, which allows the reassembly of the soluble protein into particles in vitro. Analysis of the dialyzed protein on a 5 to 25% sucrose gradient prepared in 0.1 M phosphate buffer, pH 6, revealed two peaks of radioactivity, corresponding to 23- and

TABLE 1. Biochemical properties of 23- and 38-nm VLPs

| Biochemical property | Results with VLPs | |
|---|---|---|
| | 23 nm | 38 nm |
| Immunoprecipitation by polyclonal RαrNV[a] | Yes | Yes |
| Immunoprecipitation by MAbs NV8812, NV7411 and NV8301[b] | Yes | Yes |
| Binding to Caco-2 cells in culture[c] | Yes; competition with 38-nm VLPs | Yes |
| Trypsin treatment of VLPs | Resistant | Resistant |
| Trypsin treatment of alkali-dissociated VLPs[d] | 32K cleavage product | 32K cleavage product |

[a] RαrNV, hyperimmune rabbit anti-rNV serum (18).
[b] MAbs NV8812, NV7411, and NV8301 recognize conformational epitopes at the C-terminal 302 residues (12).
[c] Data reported previously (28).
[d] Trypsin cleaves the NV capsid protein at residue 227, yielding a major product of 32K corresponding to the C-terminal residues 228 to 530 (13).

38-nm VLPs (Fig. 3C), as confirmed by electron microscopic analysis of an aliquot of the dialyzed material before sucrose gradient centrifugation (Fig. 3F). SDS-PAGE of the in vitro-reassembled 23- and 38-nm VLPs indicated that the 58K protein and the smaller fragments of the capsid protein were incorporated into the two types of VLPs in the same proportion (data not shown). Since the precise nature of the soluble intermediates in the alkaline dissociation of the 23-nm VLPs is unknown, we do not know whether these cleaved fragments were incorporated as monomers into the growing capsids or as part of larger intermediates that were incompletely disassembled. We currently are investigating the composition of the disassembly intermediates to address this question. However, the reassembly of particles of both sizes suggest that the alkaline treatment of the 23-nm VLPs generates soluble intermediates that are building blocks in the assembly of both 23- and 38-nm VLPs. We hypothesize that these soluble intermediates are oligomers that tolerate N-terminal cleavage of their component capsid proteins probably because those cleavages do not affect dimerization and the protein-protein interactions required for assembly of both types of VLPs. The results also indicate that the conditions used in our reassembly assay were favorable for the formation of both structures. It has been observed that when the 38-nm VLPs are dissociated under the same conditions (data not shown), more than 98% of the reassembled VLPs are 38 nm in diameter, suggesting that the type of VLP that is dissociated affects the ratio of reassembled VLPs. Since the nature and composition of the soluble intermediates may also determine the ratio of reassembled particles, further characterization of the intermediate products of the alkaline dissociation will facilitate understanding of how alternative pathways are selected.

**Antigenic and biochemical properties of the 23- and 38-nm VLPs are similar.** Having demonstrated that the 58K full-length capsid protein is the major component of both 23- and 38-nm VLPs and that the building blocks in the assembly of both structures are common, we proceeded to examine whether the capsid proteins in the two structures have the same properties regarding antigenic domains and susceptibility to trypsin cleavage. These data should provide some insight into the degree of conservation of the tertiary and quaternary folding of the capsid protein in each structure.

The antigenic properties of the 23-nm VLPs were compared to those of the 38-nm VLPs by analyzing the reactivities of both types of particles with polyclonal and monoclonal (MAb) antibodies to rNV VLPs by immunoprecipitation. The results are summarized in Table 1. Radiolabeled 23- or 38-nm VLPs were immunoprecipitated under nondenaturing conditions with rabbit polyclonal hyperimmune antisera to rNV VLPs that behave as type-specific sera based on the lack of reactivity with NV-related viruses in enzyme-linked immunosorbent assay (19) and with each of the following rNV MAbs: NV8812, NV7411, and NV8301, diluted 1:50 and 1:100 as described elsewhere (28). These MAbs have been shown to recognize discontinuous epitopes on the C-terminal 302 residues of the NV capsid protein (12). Polyclonal antibodies and MAbs were able to immunoprecipitate the 58K capsid protein in both the 38- and the 23-nm particles as well as the cleaved fragments in the 23-nm VLP preparations (data not shown). These results indicate that the immunodominant epitopes on the capsid protein as well as the conformational epitopes recognized by these MAbs are conserved in the two types of particles.

We also tested the susceptibility of the capsid protein in particulate form and in soluble form to trypsin treatment. The NV capsid protein in the 38-nm VLPs is resistant to trypsin cleavage, but if the VLPs are pretreated with alkali to dissociate them into soluble protein, the trypsin cleavage site at residue 227 becomes exposed, and trypsin cleavage at residue 227 results in a 32K fragment of residues 228 to 530 (13). $^{35}$S-radiolabeled 38- and 23-nm VLPs (0.2 μg/μl) were treated for 5 min with 10 mM Tris, pH 8.9, at room temperature to partially dissociate the VLPs. The particles were then subjected to sucrose gradient centrifugation to separate the soluble capsid protein from the protein assembled in VLPs. Two peaks of radioactivity corresponding to dissociated (banding at the top of the gradient) and particulate (banding at the middle of the gradient) NV capsid protein were detected in gradients of both 23- and 38-nm VLPs. Aliquots from each peak were treated with 10 μg of *N*-tosyl phenylalanine chloromethyl ketone (Worthington Biochemical, Freehold, N.J.) for 30 min at 37°C and then analyzed by SDS-PAGE. The capsid protein in the 23-nm VLPs showed the same behavior upon trypsin treatment as did the 38-nm VLPs (Table 1). The capsid protein was resistant to cleavage when in a particle, while the dissociated protein was susceptible to digestion, yielding a 32K cleavage product. These results indicate that the trypsin cleavage site at position 227 is protected in both structures, becoming exposed only after alkaline dissociation of VLPs.

We have demonstrated previously that the domain on the capsid protein responsible for specific binding to cells in culture (residues 300 to 384) is conserved in the two structures by showing that purified 23-nm VLPs were able to compete with the 38-nm VLPs for specific binding sites on the surface of differentiated human intestinal cells (Caco-2) grown in cultures (28). The conservation of conformational antigenic domains, trypsin cleavage susceptibility, and cell binding activity suggests that the capsid protein in the small particles may fold into a tertiary structure similar to the 38-nm VLPs. Atomic-resolution structural data will confirm this hypothesis.

The data presented in this paper indicate that the capsid

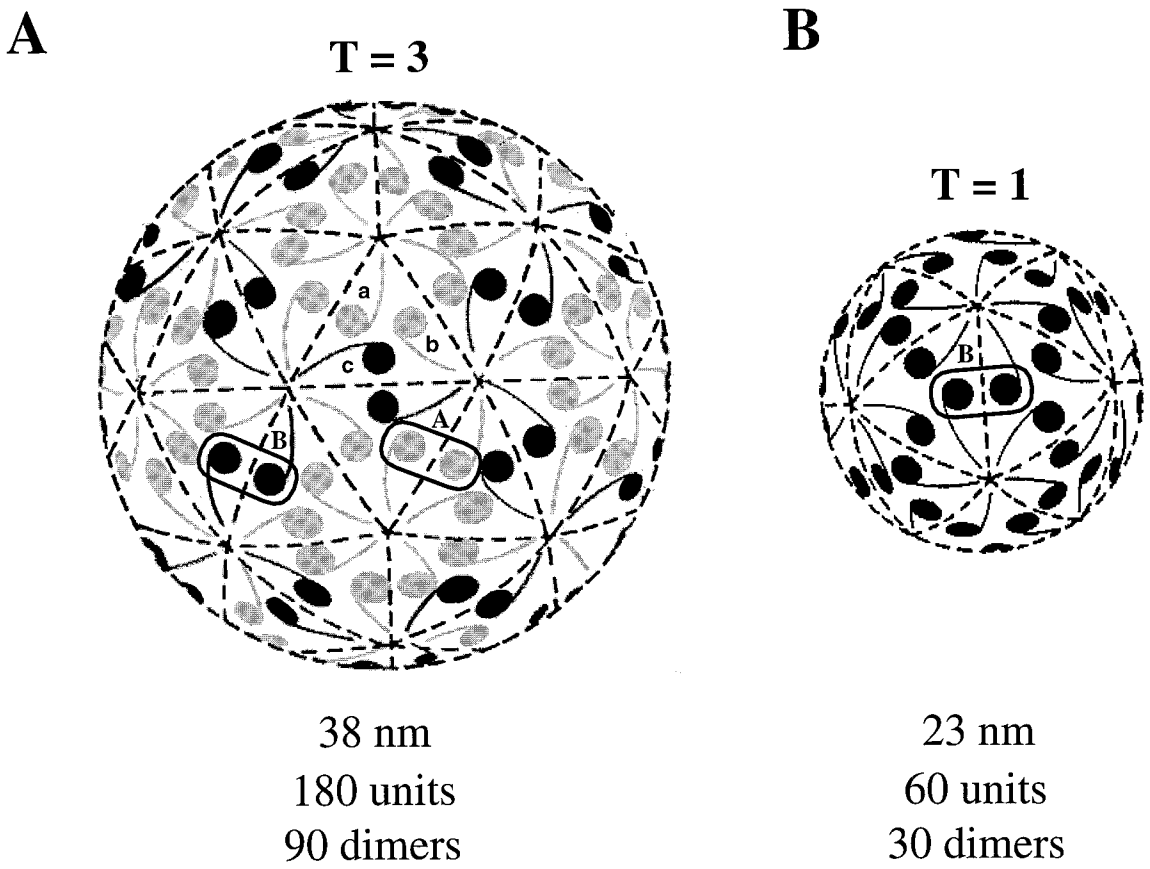


FIG. 4. Schematic representation of virus capsids with T=3 and T=1 icosahedral symmetries. (A) The T=3 capsid structure of the 38-nm rNV VLPs and other single-stranded RNA small spherical viruses (16) is formed by 180 molecules of the capsid protein; each protein molecule is represented by a comma-like symbol. The subunits are chemically identical, but intersubunit contacts differ depending on subunit location in the shell (a, b, or c). The 180 subunits are arranged as 90 dimers of two types: 60 A dimers (quasiequivalent; shaded commas) surround the icosahedral fivefold axis, and 30 B dimers (equivalent; solid commas) are located at the strict twofold axis of the icosahedral structure (23). (B) The predicted T=1 structure of the 23-nm VLPs would be formed by 60 units of the capsid protein arranged as 30 dimers (solid commas) surrounding the fivefold axis. (Modified from an article by Harrison [15], with permission of Elsevier Science Ltd.)

protein of NV, a calicivirus with T=3 icosahedral symmetry, has the structural flexibility to assemble into an alternate structure in the absence of RNA. This alternate structure of 23 nm in diameter exhibits antigenic domains, patterns of protection to trypsin cleavage, and cell binding sites similar to those of the T=3 particle; it is formed predominantly by full-length capsid protein that assembles through oligomeric intermediates that are common to the in vitro assembly pathway of particles of both sizes. Based on our data, we predict that the capsid protein in both types of VLPs folds into the same domains and that the different structures result from different subunit interactions during assembly. The observed size of the small particles corresponds to that expected for a T=1 structure formed by a capsid protein of 58 kDa that forms a T=3 structure of 38 nm. We predict that the 23-nm VLPs would be formed when 60 units of the capsid protein assembles into a structure with T=1 symmetry (Fig. 4). We propose that dimers of the capsid protein are common intermediates in the assembly of both types of particles and that during assembly the dimers adopt different orientations that result in different structures. Mass density calculations and the location and shape of the capsomers indicate that these represent dimers of the capsid protein, suggesting that preformed dimers might be the building blocks in the assembly of the rNV VLPs (24).

The three-dimensional structure of the rNV VLPs shows two types of capsomers or dimers based on their locations with respect to the icosahedral axes of symmetry. Sixty A dimers surround the icosahedral fivefold axes, and 30 B dimers are located at the strict twofold axes of the icosahedral structure (Fig. 4A). The two sides of a B dimer are equivalent as they are related to one another by the strict twofold axes, while the two sides of the type A arch are not strictly equivalent since they are related by the local twofold axes. This is also true for other spherical RNA plant viruses (tomato bushy stunt virus and SBMV) whose structures are known at atomic resolution (reviewed in reference 16). In these T=3 plant viruses, the N-terminal arm sequence is ordered only in the 30 B dimers, which create a flatter surface than the A dimers (16). In the predicted T=1 structure of the 23-nm VLPs, all the dimers would be equivalent to each other and would be located at the icosahedral twofold axis, surrounding the fivefold axis (Fig. 4B).

The 58K protein in the 23-nm VLPs undergoes N-terminal cleavage upon storage (Fig. 2B) more readily than the 38-nm VLPs. This different susceptibility to cleavage may be the result of the different organization of the N-terminal residues in the 23-nm VLPs compared to that in the T=3 38-nm VLPs. According to our hypothesis, all the monomers constituting the dimers in the 23-nm VLPs are equivalent, and the N-terminal residues would be equally susceptible to degradation. Our ob-

servations would be explained if the N-terminal residues within the B dimers in the 23-nm particles are more susceptible to degradation than the N-terminal residues in the A dimers that are present in the 38-nm VLPs but absent in the smaller structures. The higher susceptibility of the 58K protein in the 23-nm VLPs does not seem to be associated with instability of the particles, since particles with the cleaved pattern (Fig. 2B) are stable at 4°C for several months.

It has been shown that the N-terminal arm of the capsid proteins of SBMV, alfalfa mosaic virus, and brome mosaic virus is not necessary for the assembly of T=1 icosahedral particles when these residues are removed by trypsin treatment (4, 9, 16, 25). These observations agree with our results and suggest that the residues in the N terminus of the NV capsid protein may not be essential for the assembly of T=1 structures. Experiments are in progress to analyze the ability of N-terminally truncated mutants of the capsid protein to assemble into T=1 and T=3 particles.

The mechanism that controls the ability of the dimers to assemble into larger or smaller structures is still unknown for NV. The structure of small icosahedral plant viruses seen at high resolution shows that the flexibility in those viruses is built into the subunit contacts (1, 6, 7, 15). In the case of SBMV, it has been reported that the formation of T=3 and T=1 particles at low ionic strength from isolated SBMV coat protein and RNA might be regulated by the charge configuration of carboxyl group clusters in the putative initiation complex, a 10-mer or pentamer of dimers, which is common in the morphogenesis of both structures. The charge configuration, which is modulated by pH, divalent cations, and the presence of the arm domain, regulates further subunit interactions and hence the mode of T=3 versus T=1 assembly (7, 25).

The occurrence of particles of two sizes (35 to 40 and 15 to 20 nm in diameter) with a similar morphology in stool samples from patients infected with a human calicivirus, the Otofuke agent (27), suggests that the dimorphism described here is not an artifact caused by the overexpression of the capsid protein in insect cells.

Viral particles of two sizes (25 to 27 and 32 to 40 nm in diameter) have also been found in liver homogenates of rabbits and hares infected with one of two animal caliciviruses, rabbit hemorrhagic disease virus (RHDV) and European brown hare syndrome virus (3). These caliciviruses are responsible for an acute and fatal hepatitis of adult rabbits. However, the smaller particles, or core-like particles (CLPs), are composed of a 30K protein that has been reported to represent the N terminus of the capsid protein (2, 3, 10). These particles appear smooth by negative-stain electron microscopy and show different antigenic properties relative to the RHDV virions by immunoblotting and immunoelectron microscopy (10). The RHDV virions with a diameter of 32 to 40 nm are formed by the full-length capsid protein (VP60) and have typical calicivirus morphology with cup-like depressions. The characteristics of the small CLPs suggest that they are formed by a different mechanism than that for the 23-nm rNV VLPs described in this paper. The RHDV CLPs may be formed after proteolytic cleavage of the RHDV virions (3) or by expression of a truncated capsid protein (10), resulting in smooth, archless structures. It is likely that in these smaller structures for RHDV, the absence of the C-terminal domain of the capsid protein, and hence the absence of arch-like structures, accounts for the smaller diameter.

The in vivo significance of the assembly of smaller NV particles in the intestine in infected individuals is not clear. Now that it is clear that the NV capsid protein can form VLPs of two sizes, it will be of interest to see if such particles are detected and reported more frequently in clinical samples. We speculate that the smaller particles may originate in the intestinal lumen, which may provide the conditions for the reassembly of the smaller forms from alkaline-dissociated particles. These particles are likely noninfectious since they appear empty in negative-stain electron microscopy and size restrictions of these smaller particles may not permit encapsidation of a full-length genome. The ratio of smaller to typical-size particles will determine the particle/PFU ratio and may affect the infectivity of the virus; this may vary among individuals depending on differences in local conditions along the intestine. In the livers of rabbits infected with the calicivirus RHDV, the proportion of the small particles (CLPs) to the typical calicivirus particles has been associated with the course of the disease and the age of the rabbits. In acute rabbit hemorrhagic disease, few CLPs have been detected relative to the high number of typical calicivirus particles. On the other hand, protracted disease has been associated in young rabbits with the production of CLPs only (10). It will be of interest to determine whether the presence and relative proportion of smaller NV particles in infected individuals have any impact on the outcome of the disease.

The in vitro disassembly-reassembly system developed will be used to address how factors such as pH, divalent-cation concentration, and ionic strength affect the assembly of one structure versus the other. Additionally, electron cryomicroscopy techniques will be used to determine the triangulation number and other structural properties of these particles. The biochemical and structural characterization of assemblies such as 23-nm rNV VLPs will contribute to our understanding of the protein interactions that govern the assembly of small icosahedral viral capsids, as well as the factors that control the structural flexibility during assembly in vivo.

The potential uses of rNV VLPs as carriers to deliver heterologous epitopes to the mucosal sites of the immune system, or as intracellular carriers of heterologous genes, will be aided by a thorough understanding of the mechanisms by which the NV capsid protein assembles into different structures and by the identification of the domains involved in the protein-protein interactions in morphogenesis of these capsids.

We thank B. V. V. Prasad for helpful discussions, Glenn Decker for valuable assistance in electron microscopy, and Jeff Lawton for kind help with computer graphics.

This work was supported by Public Health Service grants AI-30448, AI-38036, and T32 DK-07664-03 from the National Institutes of Health and by Texas Advanced Technology Program grants 004949-033 and 004949-055.

## REFERENCES

1. **Abad-Zapatero, C., S. S. Abdel-Meguid, J. E. Johnson, A. G. W. Leslie, I. Rayment, M. G. Rossmann, D. Suck, and T. Tsukihara.** 1980. Structure of southern bean mosaic virus at 2.8 angstrom resolution. Nature **286:**33–39.
2. **Capucci, L., G. Frigoli, L. Ronshold, A. Lavazza, E. Brocchi, and C. Rossi.** 1995. Antigenicity of the rabbit hemorrhagic disease virus studied by its reactivity with monoclonal antibodies. Virus Res. **37:**221–238.
3. **Capucci, L., M. T. Scicluna, and A. Lavazza.** 1991. Diagnosis of viral haemorrhagic disease of rabbits and the European brown hare syndrome. Rev. Sci. Tech. Off. Int. Epizoot. **10:**347–370.
4. **Cuillel, M., B. Jacrot, and M. Zulauf.** 1981. A T = 1 capsid formed by protein of brome mosaic virus in the presence of trypsin. Virology **110:**63–72.
5. **Dingle, K. E., P. R. Lambden, E. O. Caul, and I. N. Clarke.** 1995. Human enteric *Caliciviridae*: the complete genome sequence and expression of virus-like particles from a genetic group II small round structured virus. J. Gen. Virol. **76:**2349–2355.
6. **Erickson, J. W., and M. G. Rossmann.** 1982. Assembly and crystallization of a T = 1 icosahedral particle from trypsinized southern bean mosaic virus coat protein. Virology **116:**128–136.
7. **Erickson, J. W., A. M. Silva, M. R. N. Murthy, I. Fita, and M. G. Rossmann.** 1985. The structure of a T = 1 icosahedral empty particle from southern bean mosaic virus. Science **229:**625–629.

8. **Estes, M. K., and M. E. Hardy.** 1995. Norwalk virus and other enteric caliciviruses, p. 1009–1034. *In* M. Blaser, P. Smith, J. Ravdin, H. B. Greenberg, and R. Guerrant (ed.), Infections of the gastrointestinal tract. Raven Press, New York, N.Y.
9. **Fukuyama, K., S. S. Abdel-Meguid, and M. G. Rossmann.** 1981. Crystallization of alfalfa mosaic virus coat protein as a T = 1 aggregate. J. Mol. Biol. **150:**33–41.
10. **Granzow, H., F. Weiland, H.-G. Strebelow, C. M. Liu, and H. Schirrmeier.** 1996. Rabbit hemorrhagic disease virus (RHDV): ultrastructure and biochemical studies of typical and core-like particles present in liver homogenates. Virus Res. **41:**163–172.
11. **Hardy, M. E., S. F. Kramer, J. J. Treanor, and M. K. Estes.** Human calicivirus genogroup II capsid sequence diversity revealed by sequence analyses of the prototype Snow Mountain Agent. Arch. Virol., in press.
12. **Hardy, M. E., T. N. Tanaka, N. Kitamoto, L. J. White, J. M. Ball, X. Jiang, and M. K. Estes.** 1996. Antigenic mapping of the recombinant Norwalk virus capsid protein using monoclonal antibodies. Virology **217:**252–261.
13. **Hardy, M. E., L. J. White, J. M. Ball, and M. K. Estes.** 1995. Specific proteolytic cleavage of recombinant Norwalk virus capsid protein. J. Virol. **69:**1693–1698.
14. **Hardy, M. E., L. J. White, and M. K. Estes.** 1996. *In vitro* assembly of the Norwalk virus capsid protein. Presented at the Keystone Symposia in Viral Genome Replication, Tamarron, Colo., 1 to 7 March 1996.
15. **Harrison, S. C.** 1984. Multiple modes of subunit association in the structures of simple spherical viruses. Trends Biochem. Sci. **9:**345–351.
16. **Harrison, S. C., J. J. Skehel, and D. C. Wiley.** 1996. Virus structure, p. 59–99. *In* B. N. Fields, D. M. Knipe, P. M. Howley, R. M. Chanock, J. L. Melnick, T. P. Monath, B. Roizman, and S. E. Straus (ed.), Fields virology. Lippincott-Raven Publishers, Philadelphia, Pa.
17. **Jiang, X., D. O. Matson, G. M. Ruiz-Palacios, J. Hu, J. Treanor, and L. K. Pickering.** 1995. Expression, self-assembly, and antigenicity of a Snow Mountain Agent-like calicivirus capsid protein. J. Clin. Microbiol. **33:**1452–1455.
18. **Jiang, X., M. Wang, D. Y. Graham, and M. K. Estes.** 1992. Expression, self-assembly, and antigenicity of the Norwalk virus capsid protein. J. Virol. **66:**6527–6532.
19. **Jiang, X., J. Wang, and M. K. Estes.** 1995. Characterization of SRSVs using RT-PCR and a new antigen ELISA. Arch. Virol. **140:**363–374.
20. **Jiang, X., M. Wang, K. Wang, and M. K. Estes.** 1993. Sequence and genomic organization of Norwalk virus. Virology **195:**51–61.
21. **Leite, J. P. G., T. Ando, J. S. Noel, B. Jiang, C. D. Humphrey, J. F. Lew, K. Y. Green, R. I. Glass, and S. S. Monroe.** 1996. Characterization of Toronto virus capsid protein expressed in baculovirus. Arch. Virol. **141:**865–875.
22. **Numata, K., M. E. Hardy, S. F. Kramer, S. Nakata S. Chiba, and M. K. Estes.** 1996. Molecular characterization of human calicivirus Sapporo. Arch. Virol., in press.
23. **Olson, N. H., and T. S. Baker.** 1989. Magnification calibration and the determination of the spherical virus diameters using cryo-microscopy. Ultramicroscopy **30:**281–298.
24. **Prasad, B. V. V., R. Rothnagel, X. Jiang, and M. K. Estes.** 1994. Three-dimensional structure of baculovirus-expressed Norwalk virus capsids. J. Virol. **68:**5117–5125.
25. **Savithri, H. S., and J. W. Erickson.** 1983. The self-assembly of the cowpea strain of southern bean mosaic virus: formation of T = 1 and T = 3 nucleoprotein particles. Virology **126:**328–335.
26. **Sorger, P. K., P. G. Stockley, and S. C. Harrison.** 1986. Structure and assembly of turnip crinkle virus. II. Mechanism of reassembly *in vitro*. J. Mol. Biol. **191:**639–658.
27. **Taniguchi, K., S. Urasawa, and T. Urasawa.** 1981. Further studies of 35-40 nm virus-like particles associated with outbreaks of acute gastroenteritis. J. Med. Microbiol. **14:**107–118.
28. **White, L. J., J. M. Ball, M. E. Hardy, T. N. Tanaka, N. Kitamoto, and M. K. Estes.** 1996. Attachment and entry of recombinant Norwalk virus capsids to cultured human and animal cell lines. J. Virol. **70:**6589–6597.